RAA 2016 Vol. **16** No. **1**, 16 (10pp) doi: 10.1088/1674–4527/16/1/016
http://www.raa-journal.org *http://iopscience.iop.org/raa*

***R**esearch in*
***A**stronomy and*
***A**strophysics*

f and g series solutions to a post-Newtonian two-body problem with parameters β and γ

Song-He Qin, Jing-Xi Liu, Ze-Hao Zhong and Yi Xie

School of Astronomy and Space Science, Nanjing University, Nanjing 210093, China; *yixie@nju.edu.cn*
Shanghai Key Laboratory of Space Navigation and Position Techniques, Shanghai 200030, China
Key Laboratory of Modern Astronomy and Astrophysics, Nanjing University, Ministry of Education, Nanjing 210093, China

Received 2015 May 14; accepted 2015 June 27

Abstract Classical Newtonian f and g series for a Keplerian two-body problem are extended for the case of a post-Newtonian two-body problem with parameters β and γ. These two parameters are introduced to parameterize the post-Newtonian approximation of alternative theories of gravity and they are both equal to 1 in general relativity. Up to the order of 30, we obtain all of the coefficients of the series in their *exact* forms without any cutoff for significant figures. The f and g series for the post-Newtonian two-body problem are also compared with a Runge-Kutta order 7 integrator. Although the f and g series have no superiority in terms of accuracy or efficiency at the order of 7, the discrepancy in the performances of these two methods is not quite distinct. However, the f and g series have the advantage of flexibility for going to higher orders. Some examples of relativistic advance of periastron are given and the effect of gravitational radiation on the scheme of f and g series is evaluated.

Key words: gravitation – celestial mechanics – binaries: general

1 INTRODUCTION

In classical Newtonian celestial mechanics, the f and g series (the Taylor's series in the time domain) can trace their history back to Lagrange in 1782. He made use of them to calculate the power series solution of Keplerian motion up to fifth order. Since then, a large amount of studies have been done on them and the series are widely used in orbit determination, interpolation of states between time steps and integration of the equations of motion for two bodies.

The radius of convergence of the f and g series for a Keplerian two-body problem in time intervals was investigated and given by Moulton (1903) and Taff (1985). The series was explicitly expressed up to 8th order by Escobal (1965). By developing a computer program which could generate and manipulate symbolic mathematical expressions, Sconzo et al. (1965) derived explicit expressions for the coefficients of the f and g series for Keplerian motion up to 27th order: the integer coefficients of terms up to 12th are exact; beyond that order, the coefficients are obtained in floating point form with eight significant figures. Bem & Szczodrowska-Kozar (1995) gave a table of the coefficients of the f and g series up to the 20th order and paid special attention to test the series in highly eccentric orbits.

The f and g series are also extended to a more general form. They could be utilized in studies on dynamics of the restricted 3-body problem (Steffensen 1956, 1957; Rabe 1961; Deprit & Price 1965), the N-body problem (Broucke 1971; Black 1973; Papadakos 1983), motion of comets (Sitarski 1979), the Solar System planets (Le Guyader 1993; Bem & Szczodrowska-Kozar 1995) and spacecrafts (Soong & Paul 1971; Sharifi & Seif 2011; Pellegrini et al. 2014).

Recently, thanks to rapid developments in technology of measurement and metrology, Einstein's general relativity (GR) needs to be employed in some cases of astrometry and celestial mechanics. Among them, the relativistic gravitational two-body problem in the parameterized post-Newtonian (PPN) formalism has been well studied. In the PPN formalism, some specific parameters are introduced to parameterize the post-Newtonian (PN) approximation of alternative theories of gravity (see Will 1993, 2006, for reviews). Therefore, as a natural step to generalize the methodology in classic Newtonian celestial mechanics to relativistic celestial mechanics, we will try to obtain the f and g series solutions to a PN two-body problem with PPN parameters β and γ. When these two parameters are both equal to 1, the series can return to those series for a PN two-body problem in GR. We derive the coefficients of these PPN f and g series for the two-body problem up to the 30th order. All of the coefficients are *exact* and can be found on *http://www.raa-journal.org/docs/Supp/2318supplement.rar.*

In Section 2, we will present the details of calculating the f and g series for a PN two-body problem with PPN parameters β and γ. The recursion formulas of these series

will also be given. Numerical validation will be checked by testing the conservation laws of energy and angular momentum in the system in Section 3. The comparison between the f and g series and a Runge-Kutta order 7 (RK7) integrator will be described as well. In Section 4, we give some examples of relativistic advance of periastron and evaluate the effect of gravitational radiation on the scheme of f and g series for a realistic two-body system. The conclusions and discussion will be presented in Section 5.

2 f AND g SERIES OF THE PPN TWO-BODY PROBLEM

In the PPN formalism, the equations of motion for a two-body problem with point masses m_1 and m_2 can be written as (Soffel et al. 1987; Brumberg 1991; Will 1993)

$$\frac{\mathrm{d}^2\boldsymbol{r}}{\mathrm{d}t^2} = \boldsymbol{a}_{\mathrm{N}} + \boldsymbol{a}_{\mathrm{PPN}}\,, \tag{1}$$

where $\boldsymbol{r}$ is the Euclidian vector from m_2 to m_1. With the definition $G = 1$ and $\epsilon \equiv c^{-1}$, the Newtonian acceleration $\boldsymbol{a}_{\mathrm{N}}$ and the PPN acceleration $\boldsymbol{a}_{\mathrm{PPN}}$ are, respectively,

$$\boldsymbol{a}_{\mathrm{N}} = -\frac{m}{r^3}\boldsymbol{r}, \tag{2}$$

$$\boldsymbol{a}_{\mathrm{PPN}} = \epsilon^2\frac{m}{r^3}\boldsymbol{r}\left[(2\beta+2\gamma+2\eta)\frac{m}{r} - (\gamma+3\eta)v^2 + \frac{3}{2}\eta\left(\frac{\boldsymbol{r}\cdot\boldsymbol{v}}{r}\right)^2\right] + \epsilon^2(2\gamma+2-2\eta)\frac{m}{r^2}\left(\frac{\boldsymbol{r}\cdot\boldsymbol{v}}{r}\right)\boldsymbol{v}\,, \tag{3}$$

where $m = m_1 + m_2$, $\mu = m_1m_2/m$, $\eta = \mu/m$ and $\boldsymbol{v} = \mathrm{d}\boldsymbol{r}/\mathrm{d}t$.

In the acceleration $\boldsymbol{a}_{\mathrm{PPN}}$, we take the PPN parameters β and γ into account and leave other PPN parameters untouched. Within the PPN formalism (see Will 1993, 2006, for reviews), γ describes the amount of space-curvature produced by unit rest mass; and β represents the nonlinearity in the superposition law for gravity. They are both equal to 1 in GR. Experiments show their deviations from 1 are very small: $|\gamma - 1| \lesssim 10^{-5}$ (Bertotti et al. 2003) and $|\beta - 1| \lesssim 10^{-4}$ (Williams et al. 2004).

In the PN two-body problem with PPN parameters β and γ, there exist integrals of motion: PPN energy E and angular momentum $\boldsymbol{L}$ (Soffel et al. 1987; Brumberg 1991; Will 1993):

$$E = \mu\Big(\frac{1}{2}\boldsymbol{v}^2 - \frac{m}{r}\Big) + \mu\epsilon^2\bigg\{\frac{3}{8}(1-3\eta)\boldsymbol{v}^4 + \frac{1}{2}(2\gamma+\eta+1)v^2\frac{m}{r} + \frac{1}{2}\eta\frac{m}{r}\Big(\frac{\boldsymbol{r}\cdot\boldsymbol{v}}{r}\Big)^2 + \frac{1}{2}(2\beta-1)\frac{m^2}{r^2}\bigg\}\,, \tag{4}$$

and

$$\boldsymbol{L} = \mu(\boldsymbol{r}\times\boldsymbol{v})\Big\{1 + \epsilon^2\Big[\frac{1}{2}v^2(1-3\eta) + (2\gamma+\eta+1)\frac{m}{r}\Big]\Big\}\,. \tag{5}$$

These invariants will be used to check the accuracy of the f and g series (see Section 3.2 for details).

Because the acceleration $\boldsymbol{a}_{\mathrm{PPN}}$ *only* depends on two basis vectors $\boldsymbol{r}$ and $\boldsymbol{v}$, like the case in the Newtonian framework of $\boldsymbol{a}_{\mathrm{N}}$, we can also have f and g series as

$$\boldsymbol{r} = f\boldsymbol{r}_0 + g\boldsymbol{v}_0\,, \tag{6}$$

$$\boldsymbol{v} = \dot{f}\boldsymbol{r}_0 + \dot{g}\boldsymbol{v}_0\,, \tag{7}$$

where dot means taking a derivative with respect to time t, $\tau \equiv t - t_0$, $\boldsymbol{r}_0 = \boldsymbol{r}(t_0)$, $\boldsymbol{v}_0 = \boldsymbol{v}(t_0)$ and

$$f = \sum_{n=0}^{\infty}\frac{1}{n!}f_n(t_0;\epsilon^2,\beta,\gamma)\tau^n\,, \tag{8}$$

$$g = \sum_{n=0}^{\infty}\frac{1}{n!}g_n(t_0;\epsilon^2,\beta,\gamma)\tau^n\,. \tag{9}$$

Here, we can see that f and g must include the relativistic corrections.

The functions of f_n and g_n satisfy the relation as

$$D^n(\boldsymbol{r}) \equiv \frac{\mathrm{d}^n}{\mathrm{d}t^n}\boldsymbol{r} = f_n\boldsymbol{r} + g_n\boldsymbol{v}\,. \tag{10}$$

For the order of $n+1$, we have

$$D^{(n+1)}(\boldsymbol{r}) = f_{n+1}\boldsymbol{r} + g_{n+1}\boldsymbol{v}\,, \tag{11}$$

which can also be obtained by taking the derivative as

$$D^{(n+1)}(\boldsymbol{r}) = D(D^n(\boldsymbol{r})) = D(f_n)\boldsymbol{r} + f_n D(\boldsymbol{r}) + D(g_n)\boldsymbol{v} + g_n D(\boldsymbol{v})\,. \tag{12}$$

With the notations that

$$u \equiv \frac{1}{r}, \quad p \equiv \frac{\boldsymbol{r}\cdot\boldsymbol{v}}{r}, \quad q \equiv v^2\,, \tag{13}$$

and with the help of Equation (1), which can be re-expressed as

$$D(\boldsymbol{v}) = -mu^3\boldsymbol{r} + \epsilon^2 mu^3\boldsymbol{r}\Big[(2\beta+2\gamma+2\eta)mu - (\gamma+3\eta)q + \frac{3}{2}\eta p^2\Big] + \epsilon^2(2\gamma+2-2\eta)mu^2 p\boldsymbol{v}\,, \tag{14}$$

Equation (12) can also be written as

$$\begin{aligned} D^{(n+1)}(\boldsymbol{r}) \;=\; & \Big[D(f_n) - mu^3 g_n + \epsilon^2(2\beta+2\gamma+2\eta)m^2u^4 g_n - \epsilon^2(\gamma+3\eta)mu^3 q g_n + \frac{3}{2}\epsilon^2\eta mu^3 p^2 g_n\Big]\boldsymbol{r} \\ & + \Big[f_n + D(g_n) + \epsilon^2(2\gamma+2-2\eta)g_n mu^2 p\Big]\boldsymbol{v}\,. \end{aligned} \tag{15}$$

After comparing the above equation with Equation (11), we can work out the recursion formulas of the series as

$$f_{n+1} \;=\; D(f_n) - mu^3 g_n + \epsilon^2 g_n mu^3\Big[(2\beta+2\gamma+2\eta)mu - (\gamma+3\eta)q + \frac{3}{2}\eta p^2\Big]\,, \tag{16}$$

$$g_{n+1} \;=\; D(g_n) + f_n + \epsilon^2(2\gamma+2-2\eta)g_n mu^2 p\,. \tag{17}$$

By making use of these recursion formulas and the following relations

$$D(u) \;=\; -u^2 p, \tag{18}$$

$$D(p) \;=\; -up^2 + uq - mu^2 + \epsilon^2 mu^2\Big[(2\beta+2\gamma+2\eta)mu - (\gamma+3\eta)q + \frac{3}{2}\eta p^2\Big] + \epsilon^2(2\gamma+2-2\eta)mu^2p^2\,, \tag{19}$$

$$D(q) \;=\; -2mu^2 p + \epsilon^2 2mu^2 p\Big[(2\beta+2\gamma+2\eta)mu - (\gamma+3\eta)q + \frac{3}{2}\eta p^2\Big] + \epsilon^2 2(2\gamma+2-2\eta)mu^2 pq\,, \tag{20}$$

we calculate the coefficients of the f and g series with the help of the symbolic manipulator MAPLE [1]. It is shown that both f_n and g_n can be expressed as

$$f_n \;=\; \sum_{k=1}^{K_n}(A_k\beta + B_k\gamma + C_k\eta + D_k)\epsilon^{a_k} m^{b_k} u^{c_k} p^{d_k} q^{e_k}\,, \tag{21}$$

$$g_n \;=\; \sum_{k=1}^{K'_n}(A'_k\beta + B'_k\gamma + C'_k\eta + D'_k)\epsilon^{a'_k} m^{b'_k} u^{c'_k} p^{d_k} q^{e'_k}\,. \tag{22}$$

All these coefficients are obtained in their *exact* forms without cutting at some significant figure. Tables 1 and 2 respectively show these coefficients for f_n and g_n with $n = 0, 1, \cdots 6$ as examples. The machine-readable files, which contain coefficients up to 30th order, can be found in the Supplementary Files.

Each K_n, which is the number of terms in the summation of f_n at the order of n, has two contributions: Newtonian part N_n and PN part P_n, i.e. $K_n = N_n + P_n$. For the f series from 0 to nth order, we define $S_n = \sum_k^n K_k$ to count the total number of terms in the summation. It is also true for $K'_n = N'_n + P'_n$ and $S'_n = \sum_k^n K'_k$.

Figure 1 shows histograms for (1) N_n, P_n and K_n (top panel), (2) N'_n, P'_n and K'_n (middle panel), and (3) S_n, S'_n and $S_n + S'_n$ (bottom panel). They can tell how many terms need to be calculated in the numerical implementation, which more or less reflects the runtime for a computer. As a crude estimation, in 1-D motion, if we consider the f and g series up to 7th order, the total number of the terms needed to be collected will reach the level of $\sim 10^2$ (see the bottom panel of Fig. 1). As a comparison, an RK7 integrator roughly deals with about $5\times 11 = 55$ terms: five terms in the equations of motion [see Eq. (1) or (14)] and 11 terms for calculating the equations of motion (e.g. see Stoer & Bulirsch 2002, for details). It means that, for a PN two-body problem, the efficiency of computing f and g series with the order $n \gtrsim 7$ will be lower than the one of an RK7 integrator (see the next section for details). Although the f and g series have this disadvantage, they can go to high orders more easily than an RK integrator.

3 NUMERICAL EVALUATION

This section presents the results obtained by applying the f and g series for orbital integration in some different cases.

Table 1 PPN f_n Series for $n = 0, 1, \cdots, 6$ in the Form of Equation (21)

n	A_k	B_k	C_k	D_k	a_k	b_k	c_k	d_k	e_k
0	0	0	0	1	0	0	0	0	0
1	0	0	0	0	0	0	0	0	0
2	0	0	0	–1	0	1	3	0	0
2	2	2	2	0	2	2	4	0	0
2	0	0	1.5	0	2	1	3	2	0
2	0	–1	–3	0	2	1	3	0	1
3	0	0	0	3	0	1	4	1	0
3	–8	–8	–3	–2	2	2	5	1	0
3	0	0	–7.5	0	2	1	4	3	0
3	0	3	12	0	2	1	4	1	1
4	0	0	0	–2	0	2	6	0	0
4	0	0	0	–15	0	1	5	2	0
4	0	0	0	3	0	1	5	0	1
4	10	12	3	4	2	3	7	0	0
4	48	54	6	24	2	2	6	2	0
4	0	0	52.5	0	2	1	5	4	0
4	–8	–14	–16	–4	2	2	6	0	1
4	0	–15	–82.5	0	2	1	5	2	1
4	0	3	12	0	2	1	5	0	2
5	0	0	0	30	0	2	7	1	0
5	0	0	0	105	0	1	6	3	0
5	0	0	0	–45	0	1	6	1	1
5	–170	–200	–15	–80	2	3	8	1	0
5	–384	–492	–15	–282	2	2	7	3	0
5	0	0	–472.5	0	2	1	6	5	0
5	144	252	225	102	2	2	7	1	1
5	0	105	787.5	0	2	1	6	3	1
5	0	–45	–225	0	2	1	6	1	2
6	0	0	0	–22	0	3	9	0	0
6	0	0	0	–420	0	2	8	2	0
6	0	0	0	–945	0	1	7	4	0
6	0	0	0	66	0	2	8	0	1
6	0	0	0	630	0	1	7	2	1
6	0	0	0	–45	0	1	7	0	2
6	176	220	22	88	2	4	10	0	0
6	2610	3180	–111	1500	2	3	9	2	0
6	3840	5550	210	3660	2	2	8	4	0
6	0	0	5197.5	0	2	1	7	6	0
6	–362	–538	–280	–208	2	3	9	0	1
6	–2304	–4212	–3204	–2112	2	2	8	2	1
6	0	–945	–9450	0	2	1	7	4	1
6	144	342	504	120	2	2	8	0	2
6	0	630	3937.5	0	2	1	7	2	2
6	0	–45	–225	0	2	1	7	0	3

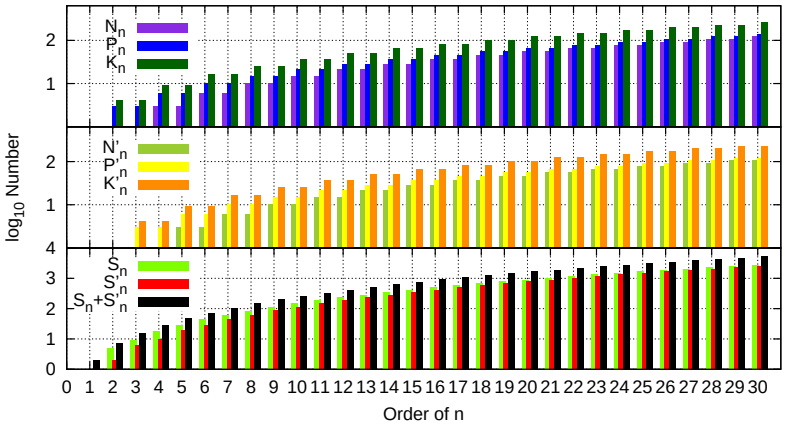

Fig. 1 Histograms on logarithmic scales for (1) N_n, P_n and K_n of the f series (*top panel*), (2) N'_n, P'_n and K'_n of the g series (*middle panel*), and (3) S_n of the f series, S'_n of the g series and $S_n + S'_n$ (*bottom panel*).

Table 2 PPN g_n Series for $n = 0, 1, \cdots, 6$ in the Form of Equation (22)

n	A'_k	B'_k	C'_k	D'_k	a'_k	b'_k	c'_k	d'_k	e'_k
0	0	0	0	0	0	0	0	0	0
1	0	0	0	1	0	0	0	0	0
2	0	2	–2	2	2	1	2	1	0
3	0	0	0	–1	0	1	3	0	0
3	2	0	4	–2	2	2	4	0	0
3	0	–6	7.5	–6	2	1	3	2	0
3	0	1	–5	2	2	1	3	0	1
4	0	0	0	6	0	1	4	1	0
4	–16	0	–22	12	2	2	5	1	0
4	0	30	–45	30	2	1	4	3	0
4	0	–12	42	–18	2	1	4	1	1
5	0	0	0	–8	0	2	6	0	0
5	0	0	0	–45	0	1	5	2	0
5	0	0	0	9	0	1	5	0	1
5	38	24	37	–8	2	3	7	0	0
5	144	12	174	–78	2	2	6	2	0
5	0	–210	367.5	–210	2	1	5	4	0
5	–24	–8	–98	26	2	2	6	0	1
5	0	135	–427.5	180	2	1	5	2	1
5	0	–9	54	–18	2	1	5	0	2
6	0	0	0	150	0	2	7	1	0
6	0	0	0	420	0	1	6	3	0
6	0	0	0	–180	0	1	6	1	1
6	–820	–536	–554	64	2	3	8	1	0
6	–1536	–288	–1860	552	2	2	7	3	0
6	0	1890	–3780	1890	2	1	6	5	0
6	576	216	1962	–444	2	2	7	1	1
6	0	–1680	5250	–2100	2	1	6	3	1
6	0	270	–1350	450	2	1	6	1	2

The validation of the series is checked. Its computational efficiency is compared with an RK7 integrator.

All numerical calculations in this work use the C compiler of the GNU Compiler Collection (GCC) v4.6.0 on a Linux Fedora 15 laptop with a quad-core Intel Core i5 CPU with 2.50 GHz clock speed and 2.8 GB of RAM.

3.1 Setup

In our simulations, we use geometrized units by setting $G = 1$ and $c = 1$ so that a quantity in terms of length can be expressed by mass (Wald 1984). Also, we only consider the cases belonging to GR after putting $\beta = \gamma = 1$. Since the angular momentum of the PN two-body system is conserved, its 3-D motion can be reduced to a planar one.

This 2-D motion can be described by the Cartesian coordinates (x, y, v_x, v_y) or the osculating orbital elements a, e, ω and f at a specific moment, where a is the semimajor axis, e is the eccentricity, ω is the argument of periastron and f is the true anomaly. We also define T_0 as its Keplerian period, which will be used to rescale the time.

Three configurations of orbits will be studied:

- A Mercury-like orbit (Orb-M) with $\beta_m \equiv m_1/m_2 = 1.660137512 \times 10^{-7}$. At the initial moment t_0, $a = 3.92172873 \times 10^7 m$, $e = 0.20563593$, $\omega = 0$ and $f = \frac{3}{2}\pi$, where $m = m_1 + m_2$.
- An Earth-like orbit (Orb-E) with $\beta_m = 3.003489650 \times 10^{-6}$. At the initial moment t_0, $a = 1.013103847 \times 10^8 m$, $e = 0.01671123$, $\omega = 0$ and $f = \frac{3}{2}\pi$, where $m = m_1 + m_2$.
- A binary pulsar PSR 0737–3039-like orbit (Orb-P) with $\beta_m = 0.8129804694$. At the initial moment t_0, $a = 2.300539153 \times 10^5 m$, $e = 0.0877775$, $\omega = 0$ and $f = \frac{3}{2}\pi$, where $m = m_1 + m_2$.

Orb-M has a relatively large eccentricity; Orb-P has a mass ratio β_m close to 1 and a smaller semimajor axis, leading to a larger relativistic correction. In fact, the relativistic periastron advances in the binary pulsar PSR 0737–3039 (Kramer et al. 2006) can exceed the corresponding value for Mercury by a factor of $\sim 10^5$.

3.2 Accuracy Check: Integrals of Motion

Integrals of motion play an important role in numerical calculations. Although Huang & Innanen (1983) pointed out that variation of the conserved integral invariants occasionally might not reflect errors in the integration, the accuracy of the method of integration can still roughly be shown by the change of an invariant. We calculate variations of the conserved PPN energy E [see Eq. (4)] and the conserved magnitude of the PPN angular momentum $\boldsymbol{L}$ [see Eq. (5)] as

$$\delta E \equiv \log_{10}\Big(\big|\frac{E - E_0}{E_0}\big|\Big), \tag{23}$$

$$\delta L \equiv \log_{10}\Big(\big|\frac{L - L_0}{L_0}\big|\Big), \tag{24}$$

where $E_0 = E(t_0)$, $L = |\boldsymbol{L}|$ and $L_0 = |\boldsymbol{L}(t_0)|$.

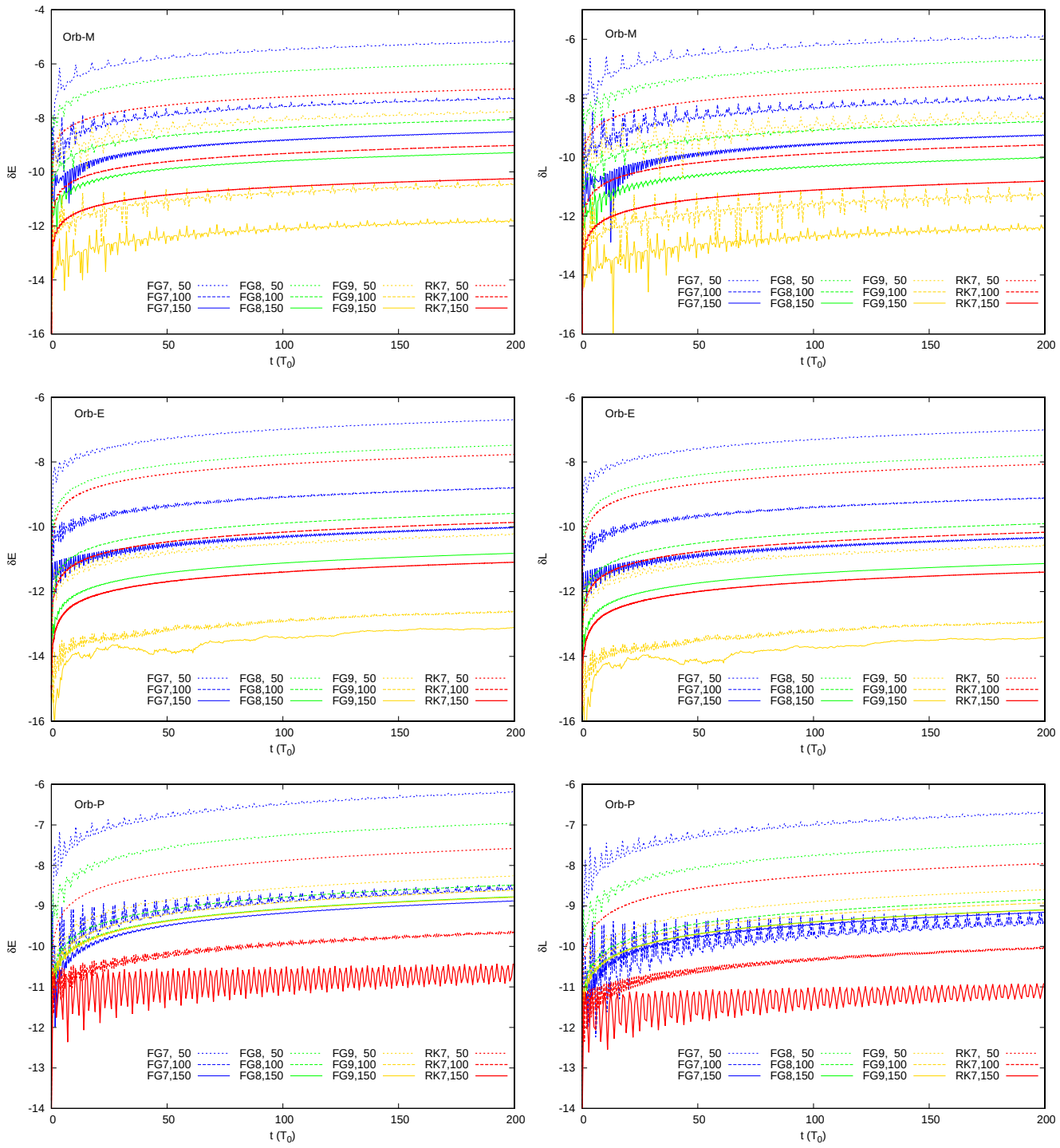

Fig. 2 Variations of δE (*left column*) and δL (*right column*) for Orb-M (*top row*), Orb-E (*middle row*) and Orb-P (*bottom row*) versus time t. The origins of all time coordinates are chosen to coincide at t_0 and the times t are represented in the unit of the Keplerian period of the system T_0. The labels of "FGn, N" mean the curves are calculated by the f and g series up to the order of n and with the step-sizes of T_0/N. The notation "RKn, N" means that this has the same order and step-size as those with "FGn, N" except for the usage of an RK7 integrator.

Figure 2 shows the variations of δE (left) and δL (right) for Orb-M (top row), Orb-E (middle row) and Orb-P (bottom row) versus time t. The origins of all time coordinates are chosen to coincide at t_0 and the times t are represented in the unit of the Keplerian period of each system T_0. The labels of "FGn,N" mean the curves are calculated by the f and g series up to the order of n and with the step-size of T_0/N. The notation "RKn,N" means that this

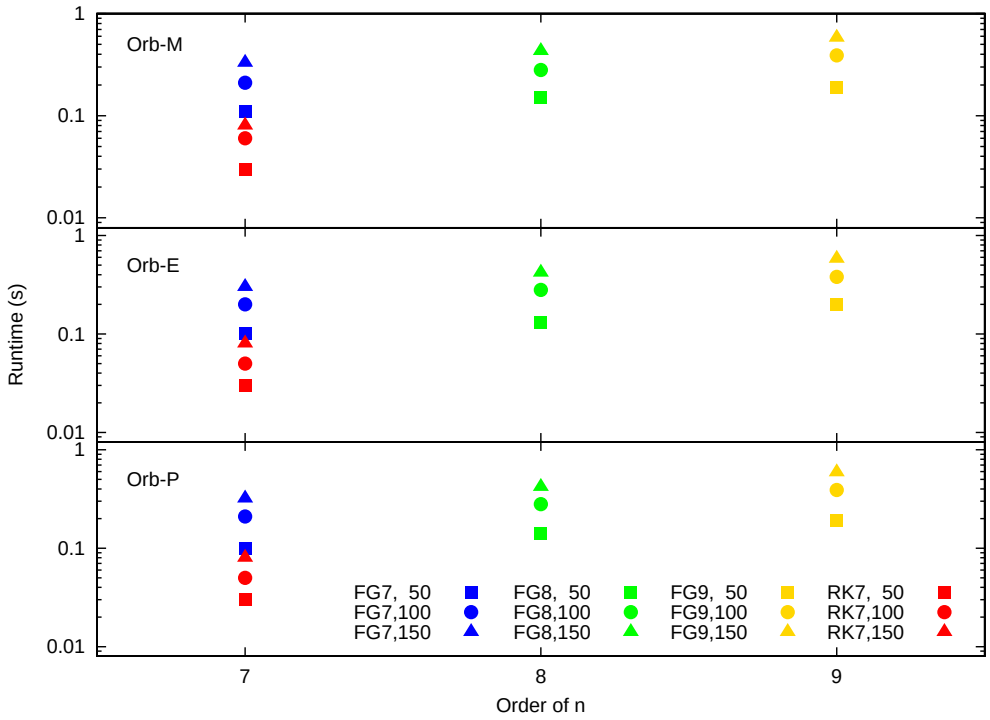

Fig. 3 Runtime of the curves in Figure 2 for Orb-M (*top row*), Orb-E (*middle row*) and Orb-P (*bottom row*) with various methods, orders and step-sizes. The labels of "FGn, N" mean the usage of the f and g series up to the order of n and with the step-sizes of T_0/N. The notation "RKn, N" means that this has the same order and step-size as those with "FGn, N" except for the usage of an RK7 integrator.

has the same order and step-size as those with "FGn,N" except for the usage of an RK integrator.

All of the figures show, at the same order $n = 7$ and with the same step-sizes, the accuracy of the f and g series is worse than that for the RK integrator by about two orders of magnitude. Although Pellegrini et al. (2014) did not directly show the same figures as ours, the maximum change and the root-mean-square of the change in the Hamiltonian (energy) for an unperturbed Keplerian two-body problem by different methods of orbital propagation under Sundman transformations were given [see fig. 4 in Pellegrini et al. (2014)]. Just like we find, it was shown by Pellegrini et al. (2014) that, with the same step-sizes, the maximum change and the root-mean-square of the change in Hamiltonian caused by RK8 were smaller than those of the f and g series of order 8 by about 2 orders of magnitude. When we use higher orders of the f and g series, such as the order of 9 for Orb-M in the top row of Figure 2 and the orders of 8 and 9 for Orb-E in the middle row of Figure 2, the accuracy can be improved to the level close to or better than that provided by RK7. The accuracy of Orb-E is more easily improved than the one of Orb-M because the relativistic correction to Orb-E is smaller. However, this tendency of improvement by increasing the order of f and g series does not work on Orb-P in the bottom row of Figure 2. It perhaps may be caused by its mass ratio ~ 1, which can enlarge the relativistic correction in Equation (1) by an increment of η in the $a_{\rm PPN}$.

3.3 Computational Efficiency: Runtime Comparisons

In order to compare the runtime of the f and g series and the RK7 integrator, we use the functions CLOCK_T and CLOCKS_PER_SEC in the C compiler to return the CPU time in seconds.

As Figure 1 indicates, the lower efficiency of computing f and g series has order $n \gtrsim 7$. The results shown in Figure 3 quantitatively confirm this. Figure 3 presents runtime of the curves in Figure 2 for Orb-M (top row), Orb-E (middle row) and Orb-P (bottom row) with various methods, orders and step-sizes. The labels of "FGn, N" mean the usage of the f and g series up to the order of n and with the step-sizes of T_0/N. The notation "RKn, N" means that this has the same order and step-size as those with "FGn, N" except for the usage of an RK7 integrator. We find that the RK7 integrator is more efficient than the f and g series in our numerical simulations on the PN two-body problems although this statement is opposite for Newtonian (Keplerian) two-body problems (Pellegrini et al. 2014). The reason is that the PN correction in the equations of motion [Eq. (1)] generates quite a lot of terms in the f and g series. Despite suffering low efficiency, the flexibility of going to higher orders is the advantage of the f and g series in the PN two-body problem.

4 ASTROPHYSICAL APPLICATIONS

In this section, we will discuss applications of the f and g series in astrophysics: relativistic advance of periastron and

some concerns about the effect of gravitational radiation on the scheme of f and g series for a realistic two-body system.

4.1 Advance of periastron

Relativistic advance of periastron is one of the most important features of a two-body problem in the framework of GR. In fact, the anomaly in the perihelion shift of Mercury (Nobili & Will 1986) gave a hint about GR and these advances of planets in the solar system have been used to test fundamental laws of physics (e.g. Iorio & Saridakis 2012; Iorio 2013; Xie & Deng 2013; Iorio 2014a,b; Li et al. 2014; Deng & Xie 2014; Liang & Xie 2014; Liu et al. 2014; Deng & Xie 2015a,b). It is also true for binary pulsars, whose advances of periastron are widely used for testing gravitational laws (e.g. Bell et al. 1996; Damour & Esposito-Farèse 1996; Kramer et al. 2006; Iorio 2007; Deng et al. 2009; Li 2010; Deng 2011; Li 2011; De Laurentis et al. 2012; Ragos et al. 2013; Xie 2013; Lu et al. 2014).

We take the results of Orb-M and Orb-P calculated by "FG7,100", "FG8,100, FG9,100" and "RK7,100" as examples for calculating the advance of periastron. The (osculating) argument of periastron ω is obtained at each step for each run and then the time series of ω is fitted according to a linear pattern $\omega = \omega_0 + \dot{\omega}t$ to show its rate, i.e. $\dot{\omega} \equiv \mathrm{d}\omega/\mathrm{d}t$. GR predicts that, up to the 1PN order, it has the value of (Misner et al. 1973; Landau & Lifshitz 1975; Brumberg 1991)

$$\dot{\omega} = 3\Big(\frac{T_0}{2\pi}\Big)^{-5/3}(Gm)^{2/3}c^{-2}(1-e^2)^{-1}\,. \tag{25}$$

Table 3 shows the fitted values of $\dot{\omega}$ of Orb-M and Orb-P by the schemes of "FGn,100" ($n = 7, 8, 9$) and "RK7,100". The theoretical values predicted by GR are also given. As has been shown in Section 3.2 for the case of Orb-M, when we use the higher orders of the f and g series, the calculated value of $\dot{\omega}$ will be effectively improved and will be closer to the theoretical value. The scheme of "FG9,100" gives a better value of $\dot{\omega}$ of Orb-M than the method of "RK7,100". In the case of Orb-P, although the trend of improvement with higher orders can still be found for the f and g series, its efficiency becomes lower than the one in the case of Orb-M and the method of "RK7,100" performs better, like what we have found in Section 3.2.

4.2 Gravitational radiation

For a realistic two-body system in the framework of GR, it emits gravitational radiation, causing its orbit to shrink (Misner et al. 1973; Landau & Lifshitz 1975). Due to the gravitational radiation, a and e will decay such that (Brumberg 1991):

$$\frac{\mathrm{d}a}{\mathrm{d}t} = -\frac{64}{5}\frac{G^3m_1m_2m}{c^5a^3(1-e^2)^{7/2}}\Big(1+\frac{73}{24}e^2+\frac{37}{96}e^4\Big)\,, \tag{26}$$

$$\frac{\mathrm{d}e}{\mathrm{d}t} = -\frac{1}{15}\frac{G^3m_1m_2m}{c^5a^4(1-e^2)^{5/2}}e(304+121e^2)\,. \tag{27}$$

The energy and angular momentum dissipate as well; up to the leading order, they change as (Brumberg 1991)

$$\frac{1}{E}\frac{\mathrm{d}E}{\mathrm{d}t} = -\frac{64}{5}\frac{G^3m_1m_2m}{c^5a^4(1-e^2)^{7/2}}\Big(1+\frac{73}{24}e^2+\frac{37}{96}e^4\Big), \tag{28}$$

$$\frac{1}{L}\frac{\mathrm{d}L}{\mathrm{d}t} = -\frac{4}{5}\frac{G^3m_1m_2m}{c^5a^4(1-e^2)^{5/2}}(8+7e^2)\,. \tag{29}$$

As rough estimates, we can have that

$$\Delta E_{\rm GW} \equiv \log_{10}\Big(\Big|\frac{E-E_0}{E_0}\Big|\Big)_{\rm GW} \approx \log_{10}\Big[\Big(\frac{1}{E}\frac{\mathrm{d}E}{\mathrm{d}t}\Big)N_ET_0\Big]\,, \tag{30}$$

$$\Delta L_{\rm GW} \equiv \log_{10}\Big(\Big|\frac{L-L_0}{L_0}\Big|\Big)_{\rm GW} \approx \log_{10}\Big[\Big(\frac{1}{L}\frac{\mathrm{d}L}{\mathrm{d}t}\Big)N_LT_0\Big]\,, \tag{31}$$

where N_E and N_L are the two numbers representing Keplerian periods. Figure 2 shows the variation of δE and δL for Orb-M, Obr-E and Orb-P. It is necessary to know when the dissipation caused by the gravitational radiation can become comparable with the one due to the truncation error of the f and g series indicated by Figure 2. If we assume $\Delta E_{\rm GW} \sim \Delta L_{\rm GW} \sim -10$, it can be found that (1) $N_E \sim N_L \sim 10^{15}$ for the case of Orb-M, (2) $N_E \sim N_L \sim 10^{15}$ for Orb-E, and (3) $N_E \sim N_L \sim 300$ for Orb-P. It means that, in the cases of planetary orbits like Orb-M and Orb-E, the gravitation radiation will not affect the validity of the f and g series because the dissipation due to gravitational radiation is much smaller than the truncation error of the f and g series in the time span $\sim 10^{15}T_0$. However, since the gravitational radiation will quickly become significant in compact binaries like Orb-P, the validities of the f and g series and 1PN approximation need to be carefully checked in their long-term dynamical evolution.

Table 3 Relativistic Advance of Periastron of Orb-M and Orb-P

	Orb-M	Orb-P
	$\dot{\omega}$ (as cy^{-1})	$\dot{\omega}$ ($^\circ$ yr^{-1})
FG7,100	41.8898808	16.8964479
FG8,100	42.9750568	16.8976391
FG9,100	42.9800189	16.8976418
RK7,100	42.9792988	16.8976420
GR^a	42.9804651	16.8994880

Notes: ^{a} Theoretical values calculated by Equation (25).

5 CONCLUSIONS AND DISCUSSION

In this work, we derive the f and g series for a PN two-body problem with PPN parameters β and γ up to the order of 30. All of the coefficients are *exact* without any cutoff for significant figures. Tables 1 and 2 respectively show these coefficients for f_n and g_n with $n = 0, 1, \cdots, 6$ as examples. The machine-readable files, which contain the coefficients up to 30th order, can be found in the Supplementary Files.

The f and g series are compared with an RK7 integrator in the aspects of accuracy (see Fig. 2) and efficiency (see Fig. 3). We find that, at the same order $n = 7$ and with the same step-sizes, the accuracy of the f and g series is worse than the one of the RK integrator by about 2 orders of magnitude; and when the higher orders are used, the accuracy can be improved to the level close to or better than the one of the RK7 integrator. The efficiency of the f and g series is lower than the one of the RK7 integrator at the same order because the series has more terms to deal with in the calculation (see Fig. 1). However, the flexibility of going to higher orders is the advantage of the f and g series in the PN two-body problem.

Astrophysical applications of the f and g series are discussed. Some examples of relativistic advance of periastron are given. We find that, in the case of planetary orbits, when we use the higher order of the f and g series, the calculated value of $\dot{\omega}$ will be effectively improved and will be closer to the theoretical value of GR. In the case of a compact binary, although the trend of improvement with higher order can still be found for the f and g series, its efficiency becomes lower. The effect of gravitational radiation on the scheme of f and g series is evaluated as well. Our estimations indicate that, in the cases of planetary orbits, the gravitational radiation will not affect the validity of the f and g series in the time span $\sim 10^{15} T_0$. However, since the gravitational radiation will quickly become significant in compact binaries, the validities of the f and g series and 1PN approximation need to be carefully checked in their long-term dynamical evolution.

One important issue, which we do not touch on in this work and we will work on in our next investigation, is regularization of the problem (see Mikkola 2008, for a brief review and references therein). The PN perturbation on the motion of Keplerian two-body problem is velocity-dependent and algorithmic regularization (Mikkola & Merritt 2006) might be applied to it.

Acknowledgements This work is funded by the National Natural Science Foundation of China (Grant No. J1210039), the Fundamental Research Funds for the Central Universities (Grant No. 20620140586) and the Opening Project of Shanghai Key Laboratory of Space Navigation and Position Techniques (Grant No.14DZ2276100).

References

Bell, J. F., Camilo, F., & Damour, T. 1996, ApJ, 464, 857
Bem, J., & Szczodrowska-Kozar, B. 1995, A&AS, 110, 411
Bertotti, B., Iess, L., & Tortora, P. 2003, Nature, 425, 374
Black, W. 1973, Celestial Mechanics, 8, 357
Broucke, R. 1971, Celestial Mechanics, 4, 110
Brumberg, V. A. 1991, Essential Relativistic Celestial Mechanics (Bristol, England and New York, Adam Hilger)
Damour, T., & Esposito-Farèse, G. 1996, Phys. Rev. D, 53, 5541
De Laurentis, M., De Rosa, R., Garufi, F., & Milano, L. 2012, MNRAS, 424, 2371
Deng, X. 2011, Science China Physics, Mechanics, and Astronomy, 54, 2071
Deng, X.-M., & Xie, Y. 2014, Ap&SS, 350, 103
Deng, X.-M., & Xie, Y. 2015a, New Astronomy, 35, 36
Deng, X.-M., & Xie, Y. 2015b, International Journal of Theoretical Physics, 54, 1739
Deng, X.-M., Xie, Y., & Huang, T.-Y. 2009, Phys. Rev. D, 79, 044014
Deprit, A., & Price, J. F. 1965, AJ, 70, 836
Escobal, P. R. 1965, Methods of Orbit Determination (New York: Wiley)
Huang, T.-Y., & Innanen, K. A. 1983, AJ, 88, 870
Iorio, L. 2007, Ap&SS, 312, 331
Iorio, L. 2013, Classical and Quantum Gravity, 30, 165018
Iorio, L. 2014a, International Journal of Modern Physics D, 23, 50006
Iorio, L. 2014b, MNRAS, 437, 3482
Iorio, L., & Saridakis, E. N. 2012, MNRAS, 427, 1555
Kramer, M., Stairs, I. H., Manchester, R. N., et al. 2006, Science, 314, 97
Landau, L. D., & Lifshitz, E. M. 1975, The Classical Theory of Fields (Oxford: Pergamon Press)
Le Guyader, C. 1993, A&A, 272, 687
Li, L.-S. 2010, Ap&SS, 327, 59
Li, L.-S. 2011, Ap&SS, 334, 125
Li, Z.-W., Yuan, S.-F., Lu, C., & Xie, Y. 2014, RAA (Research in Astronomy and Astrophysics), 14, 139
Liang, S., & Xie, Y. 2014, RAA (Research in Astronomy and Astrophysics), 14, 527
Liu, M.-Y., Zhong, Z.-H., Han, Y.-C., et al. 2014, RAA (Research in Astronomy and Astrophysics), 14, 1019
Lu, C., Li, Z.-W., Yuan, S.-F., et al. 2014, RAA (Research in Astronomy and Astrophysics), 14, 1301
Mikkola, S. 2008, in IAU Symposium, 246, IAU Symposium, ed. E. Vesperini, M. Giersz, & A. Sills, 218
Mikkola, S., & Merritt, D. 2006, MNRAS, 372, 219

Misner, C. W., Thorne, K. S., & Wheeler, J. A. 1973, Gravitation (San Francisco: W.H. Freeman and Co.)
Moulton, F. R. 1903, AJ, 23, 93
Nobili, A. M., & Will, C. M. 1986, Nature, 320, 39
Papadakos, D. N. 1983, Celestial Mechanics, 30, 275
Pellegrini, E., Russell, R. P., & Vittaldev, V. 2014, Celestial Mechanics and Dynamical Astronomy, 118, 355
Rabe, E. 1961, AJ, 66, 500
Ragos, O., Haranas, I., & Gkigkitzis, I. 2013, Ap&SS, 345, 67
Sconzo, P., Leschack, A. R., & Tobey, R. 1965, AJ, 70, 269
Sharifi, M. A., & Seif, M. R. 2011, Advances in Space Research, 48, 904
Sitarski, G. 1979, Acta Astronomica, 29, 401
Soffel, M., Ruder, H., & Schneider, M. 1987, Celestial Mechanics, 40, 77
Soong, T. T., & Paul, N. A. 1971, AIAA Journal, 9, 589
Steffensen, J. F. 1956, Acta Math, 95, 25
Steffensen, J. F. 1957, Math. Fys. Medd. Dansk. Vid. Selskap, 31, 18
Stoer, J., & Bulirsch, R. 2002, Introduction to Numerical Analysis (New York: Springer)
Taff, L. G. 1985, Celestial Mechanics: A Computational Guide for the Practitioner (New York: Wiley-Interscience)
Wald, R. M. 1984, General relativity (Chicago: University of Chicago Press)
Will, C. M. 1993, Theory and Experiment in Gravitational Physics (Cambridge: Cambridge University Press)
Will, C. M. 2006, Living Reviews in Relativity, 9, 3
Williams, J. G., Turyshev, S. G., & Boggs, D. H. 2004, Physical Review Letters, 93, 261101
Xie, Y. 2013, RAA (Research in Astronomy and Astrophysics), 13, 1
Xie, Y., & Deng, X.-M. 2013, MNRAS, 433, 3584